Nonlinear Maneuvering and Control of Ships

Roger Skjetne and Thor I. Fossen

Department of Engineering Cybernetics, Norwegian University of Science and Technology

N-7491 Trondheim, Norway. E-mail: skjetne@ieee.org, tif@itk.ntnu.no

Abstract—**We address the problem of maneuvering ships onto curves or paths in the plane. To do this, we introduce the Serret-Frenet equations and show how these fit the scope for control design with 3 degrees-of-freedom (DOF) hydrodynamic ship models in the loop. The Davidson & Schiff linear parametrically varying (LPV) ship model is used in the design, and we show how we can manipulate this by introducing acceleration feedback and by moving the body-frame freely. This simplifies the control design in such a way that we do not have to deal with zero-dynamics. Instead we use a 3-step backstepping design and theory for interconnecting subsystems. Real data from a 175 m container ship is used in a computer simulation to validate the design.** *Copyright ©2001 MTS/IEEE*

Keywords—**Ship maneuvering; Serret-Frenet frame; Plane kinematics; Backstepping; Small-gain; Acceleration feedback.**

I. INTRODUCTION

THE research area of ship maneuvering and control is a field of high interest, and the developments in the last decade in nonlinear control theory [1] greatly extends the possibilities. While ship dynamics is accurately described by complex nonlinear hydrodynamic models, the state-of-the-art models for control purposes are still simple linear models developed decades ago. Examples are the linear steering model of Davidson and Schiff [2] or the course-keeping models of Nomoto [3]. The contribution in [4] exploits the simplicity of these models, and this illustrates the need for simplicity in practical applications. More recently, ship models have appeared which written in the Euler-Lagrange form show clear connections with passive and dissipative properties of the physical system. It would be advantageous to exploit such properties in control design since an overall passive system is very robust. See [5] for a comprehensive treatise on the older models and the newer Euler-Lagrange type of models.

The problem we will address in this paper is nonlinear control of ships to predefined paths in the plane. Typically, a path is made up of waypoints with straight lines between them, and then the control system should regulate the cross-track error to zero and at the same time keep the heading towards the next waypoint [6]. What makes such a control design nontrivial is that we have to control two degrees-of-freedom by only using one actuator, namely the rudder. We will relax the requirement of waypoints and straight lines and rather develop a nonlinear controller that keeps the ship on any feasible path or curve in the plane. Within the notion of feasibility we put both geographical concerns as well as dynamic properties of the ships, e.g. its minimum turning radius. Also note that a system that manages to follow a smooth reference curve is more desirable since a smooth path is most likely to be the optimal feasible dynamic path between two points with respect to time and fuel consumption.

Supported by the Norwegian Research Council through the Strategic University Program on Marine Cybernetics

At this point we are not concerned with the dynamic model of the ship. However, we will only consider models that represent the ship dynamics in terms of surge u, sway v and yaw-rate r, and therefore we will use the linear model of Davidson and Schiff [2] in the design. This paper is the initial work of a comprehensive study of ship maneuvering, where we hope to obtain good knowledge for controlling complex hydrodynamic ship models.

Recent developments in path control have been made by [7] where they address the problem of following straight lines.To do this they redefine the output to a combination between the cross-track error and the heading angle. The result is a relative degree 2 system which is controlled by input-output linearization and robustly by sliding-mode control. Path control to straight lines, i.e. way-point tracking, has also been explored in [6] which shows a development in the output-redefinition. However, they use a very simplified dynamic model. Lately there is the work of [8] and [9] where they use a Serret-Frenet frame to represent the cross-track error and heading error. The advantage with this frame is that you move beyond straight lines and rather view the path as general smooth curves in the plane. In the last reference, they follow the same design procedure as we will do in this paper, but they use different dynamical models.

In our contribution, we will explore the Serret-Frenet frame. We will exploit the output redefinition introduced in [6]; however, with a different control strategy. Instead of using feedback linearization on a relative degree 2 problem where you get the problem of stabilizing a degree 2 zero-dynamics, we use a 3-step backstepping design and show through interconnection of subsystems and a small-gain argument that the overall plant is stable. To get to the result, we will manipulate the dynamical model by moving the body-frame and, if necessary, introducing acceleration feedback.

A. Notation

- $|\cdot|$ is the absolute value of a scalar, $|\cdot|_p$ is the *p-norm* of a vector, and $||\delta||$ denotes $ess.\sup\{|\delta(t)|, t \geq 0\}$ for any measurable signal $\delta : [0, \infty] \to \Re^m$.
- It will be clear from the context if a quantity is a scalar or vector. However, the notation $z_{1,2,...,p}$ means $[z_1, z_2, ..., z_p]^\top$.
- Differentiation w.r.t. time is denoted $\dot{x} = \frac{dx}{dt}$.
- *IOS* stands for *I*nput-*O*utput *S*table, *LAS* means *L*ocal *A*symptotic *S*tability, *L-ISS* means *L*ocally *I*nput-to-*S*tate *S*table, *L-ISpS* is the *p*ractical equavialent, *L-IOpS* is *L*ocally *I*nput-to-*O*utput *p*ractical *S*table (see [10] and [11] for details).
- We use *class-K* and *class-KL* functions as defined in [10], but note that we only define them locally.
- Kinematics involves the use of several geometrical frames. In

this paper we denote the earth fixed inertial frame as *{E}*, body-fixed frame as *{B}*, and the Serret-Frenet frame *{SF}*. Quantities have corresponding subscripts or superscripts.

- For vectors we will use the notations given in [12]; let $\eta^n_{a,b}$ denote the position vector from the origin of frame *{a}* to the origin of frame *{b}* decomposed in frame *{n}*, let $\nu^n_{a,b}$ denote the linear velocity of frame *{b}* w.r.t. frame *{a}* decomposed in frame *{n}*, and let $\omega^n_{a,b}$ be the angular velocity of frame *{b}* w.r.t. frame *{a}* decomposed in frame *{n}*.

II. Kinematics

In this section we will look into some simple concepts of curve theory [13] and how this leads to the well-known Serret-Frenet equations. Then we will develop the necessary error signals applicable for control design which therefore constitutes the kinematic equations.

A. Curve theory

Given a desired curve $\mathbf{C}(\mathbf{x_d}, \mathbf{y_d})$ with $x_d = x_d(\theta)$ and $y_d = y_d(\theta)$ where θ is an independent parametrization variable, see figure (1), let $r_d(\theta, t) = \begin{bmatrix} x_d(\theta(t)) & y_d(\theta(t)) \end{bmatrix}^T$ be

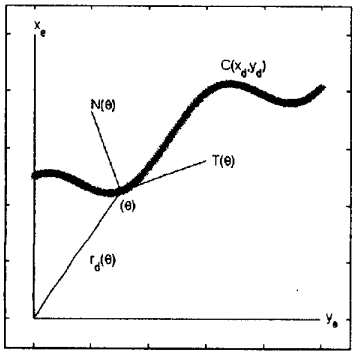

Fig. 1. Illustrates a curve $\mathbf{C}(\theta)$ with a point represented by θ and its position vector $r_d(\theta)$ and its unit tangent and normal vectors $T(\theta)$ and $N(\theta)$.

the position vector of a point on the curve at time t. Consequently, $r_d(t)$, $t \geq 0$ will be the time-evolution of a position vector with motion restricted to the curve $\mathbf{C}$. We assume that $r_d(\theta)$ is a regular parametric representation of the curve, i.e. $r_d \in C^1$ and $\frac{dr_d}{d\theta} \neq 0$ in an interval $\theta \in I$. The velocity vector is given by $v_d(t) = \dot{r}_d(t)$, and we can now express the arclength s of the curve as $\dot{s} = |v_d|$ or

$$s = \int_{\theta_0}^{\theta} \left| \frac{dr_d}{d\hat{\theta}} \right| d\hat{\theta} = \int_{\theta_0}^{\theta} \sqrt{\left(\frac{dx_d}{d\hat{\theta}}\right)^2 + \left(\frac{dy_d}{d\hat{\theta}}\right)^2}\, d\hat{\theta}$$

Consequently, either of the variables θ or s can be used to uniquely represent the curve. The expression for the *unit tangent* vector is now given by $T(t) = \frac{v_d(t)}{|v_d(t)|} = \frac{v_d(t)}{\dot{s}}$, or using the arclength, $T(s) = \frac{dr_d}{ds}$.

Remark 1: s is a natural parameter, and $r_d(s)$ is a natural representation of the curve. This is seen since $s(\theta) = \int_{\theta_0}^{\theta} \left|\frac{dr_d}{d\theta}\right| d\theta$ which implies that $\frac{ds}{d\theta} = \left|\frac{dr_d}{d\theta}\right| \rightarrow \left|\frac{dr_d}{ds}\right| = 1$. The unit tangent vector can then also be expressed by $T(s) = \frac{dr_d}{ds} = \frac{dr_d / d\theta}{|dr_d / d\theta|}$.

In the forthcomming we will use s as our parametrization variable. Let $\psi_{SF}(s)$ be the angle between the axis x_e and $T(s)$. Since $T = [T_x\ T_y]^T$ we get that $\psi_{SF}(s) = \tan^{-1}\left(\frac{T_y(s)}{T_x(s)}\right)$ which conversely gives

$$T = \begin{bmatrix} \cos(\psi_{SF}) \\ \sin(\psi_{SF}) \end{bmatrix}$$

It is interesting to see what the turning rate of T w.r.t. s is, i.e. $\frac{dT}{ds}$. We find that

$$\frac{dT}{ds} = \frac{dT}{d\psi_{SF}} \frac{d\psi_{SF}}{ds} = \begin{bmatrix} -\sin(\psi_{SF}) \\ \cos(\psi_{SF}) \end{bmatrix} \frac{d\psi_{SF}}{ds}$$

and note that $\left|\frac{dT}{ds}\right| = \left|\frac{d\psi_{SF}}{ds}\right|$. We define the *curvature vector* $K(s) := \frac{dT(s)}{ds}$ and the corresponding quantity, *curvature*, $|\kappa(s)| := |K(s)| = \left|\frac{d\psi_{SF}}{ds}\right|$, the angular scalar rate of change w.r.t. arclength s. Notice that $T^\top\left(\frac{dT}{ds}\right) = 0$ which means that the tangent and curvature vectors are orthogonal. Let ρ be some normalization factor. We can then define the *unit principal normal vector* to be $N(s) = \rho K(s)$ which is perpendicular to the tangent, and we see that $|\rho|\left|\frac{d\psi_{SF}}{ds}\right| = 1$ so $\rho = \frac{ds}{d\psi_{SF}} = \frac{1}{\kappa}$.

Remark 2: A point on the curve where $\kappa(s) = 0$ we call a *point of inflection*. At this point the curvature vector vanishes. Notice also that $K(s) = \kappa(s) N(s)$; hence, if N and K are in the same direction, then $\kappa(s) = |K(s)|$, otherwise, $\kappa(s) = -|K(s)|$. Since $N^\top N = 1$, we also get that $\kappa(s) = K^\top(s) N(s)$.

B. The Serret-Frenet equations

We are now ready to state the Serret-Frenet formulas for curves in the plane. Since $d\psi_{SF} = \kappa(s)\, ds$, we first get $\dot{\psi}_{SF} = \kappa(s)\, \dot{s}$. Moreover, we already have $\frac{dT(s)}{ds} = \kappa(s) N(s)$. The unit principal normal is given as

$$N = \begin{bmatrix} -\sin(\psi_{SF}) \\ \cos(\psi_{SF}) \end{bmatrix}$$

Then $$\frac{dN(s)}{ds} = \frac{dN}{d\psi_{SF}} \frac{d\psi_{SF}}{ds} = \kappa(s) \begin{bmatrix} -\cos(\psi_{SF}) \\ -\sin(\psi_{SF}) \end{bmatrix}$$

Summarizing, this gives

$$\frac{dT}{ds} = \kappa N \quad (1)$$

$$\frac{dN}{ds} = -\kappa T \quad (2)$$

$$\dot{\psi}_{SF} = \kappa \dot{s} \quad (3)$$

C. Serret-Frenet for control design

We will now look into the ship kinematic equations. Figure (2) shows a hypothetical scenario with all the involved frames and position vectors. Let the ship be located at $\eta^E_{E,B} = \eta = [x,\ y]^\top$ and with heading ψ as the usual jaw angle between *{B}* and *{E}*. Define the ship heading in *{SF}* as $\bar{\psi} := \psi - \psi_{SF}$, i.e. the rotational angle of *{B}* in *{SF}*. We denote a 2×2 rotation matrix as

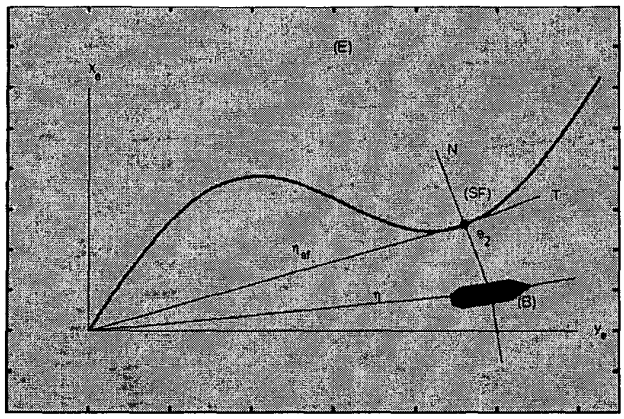

Fig. 2. Illustrates a setup with the inertial frame *{E}*, a curve **C**, a ship with frame *{B}* located at η and its projection onto the curve represented by the frame *{SF}* and the position vector η_{SF}. The cross-track error is e_2.

$$R_2(x) = \begin{bmatrix} \cos x & -\sin x \\ \sin x & \cos x \end{bmatrix}$$

and the corresponding 3×3 rotation matrix as

$$R_3(x) = \begin{bmatrix} R_2(x) & 0 \\ 0 & 1 \end{bmatrix}$$

Let the origin of *{SF}* always be the closest point on the curve from the body-fixed origin. Then the ship is located at the position $\eta_{SF,B}^{SF} = [0\ e_2]^\top$ in the *{SF}* frame, i.e. it is always located on the normal vector N with cross-track error e_2. We then get the relationship

$$\nu_{E,B}^{SF} = R_2(\bar{\psi})\,\nu_{E,B}^{B} = \nu_{E,SF}^{SF} + \nu_{SF,B}^{SF} + \omega_{E,SF}^{SF} \times \eta_{SF,B}^{SF} \quad (4)$$

where $\nu_{E,B}^{B} = [u\ v]^T$, $\nu_{E,SF}^{SF} = [\dot{s}\ 0]^\top$, $\nu_{SF,B}^{SF} = [0\ \dot{e}_2]^\top$, and

$$\omega_{E,SF}^{SF} \times \eta_{SF,B}^{SF} = \begin{bmatrix} 0 & -\dot{\psi}_{SF} \\ \dot{\psi}_{SF} & 0 \end{bmatrix} \begin{bmatrix} o \\ e_2 \end{bmatrix}$$

We also have that $\omega_{SF,B}^{SF} = \omega_{E,B}^{SF} - \omega_{E,SF}^{SF}$ or

$$\dot{\bar{\psi}} = \dot{\psi} - \dot{\psi}_{SF} = r - \dot{\psi}_{SF} \quad (5)$$

Using the Serret-Frenet equation (3) and defining the state vector $\sigma_0 = [s\ e_2\ \bar{\psi}]^\top$, the kinematics can now be written as

$$F(e_2, \kappa)\,\dot{\sigma}_0 = R_3(\bar{\psi})\,\nu_3 \quad (6)$$

where $\nu_3 = [u\ v\ r]^\top \in \{B\}$ represent the ship velocities in surge u and sway v, and yaw rate r, and

$$F(e_2, \kappa) = \begin{bmatrix} 1 - e_2\kappa & 0 & 0 \\ 0 & 1 & 0 \\ \kappa & 0 & 1 \end{bmatrix} \quad (7)$$

Definition 1: *Let the minimum possible turning radius of a given ship be denoted by R^*. This quantity is obtained in turning trials of a ship, and it is an important restriction in path generation. Correspondingly, we define $\kappa^* = 1/R^*$ as the upper bound on the curvature of the path.*

Remark 3: Notice that F is singular for $e_2 = \frac{1}{\kappa}$, which has the physical interpretation that if you are located at the center of the osculating circle[1], then the projected point on the curve will move infinitely fast. It is the task of the guidance system to provide the controller with all the signals corresponding to the curve. In this context, we should be aware that the projection algorithm within the guidance system is only well-defined if we stay within the distance $|e_2| < \left|\frac{1}{\kappa}\right|$ at all times. As a result, we will restrict the motion of e_2 by $e_2 < (1 - \lambda_1) R^*$ in the forthcomming.

III. Ship Dynamics

From above we have that the body-frame is represented by the velocities $\nu_3 = [u\ v\ r]^\top$. The 3DOF simplified equations can according to [5] be written in compact form as

$$M_3\dot{\nu}_3 + C_3(\nu_3)\,\nu_3 + D_3(\nu_3)\,\nu_3 = \tau_3 \quad (8)$$

where M_3 is the system inertia matrix, $C_3(\nu_3)$ is a matrix of coriolis and centripetal terms, $D_3(\nu_3)$ is the nonlinear system damping matrix, and τ_3 is an input of generalized forces and moments. The thrust force generated by the propellers will under the assumption of port-starboard symmetry only enter the surge mode, and consequently we can assume that surge is decoupled from the sway and yaw modes.

When moving on the path, at steady state, we wish that $u \leftrightarrow \dot{s}$, $e_2 \approx 0$, $\bar{\psi} \approx 0$, and v, r are bounded. We make the following assumptions:

(A1) *An independent control system ensures that the ship keeps a nearly constant surge speed $u \approx u_0 >> 1\,\mathrm{m/s}$.*

(A2) *The sway velocity will be bounded by the surge velocity, i.e. $\exists\ 0 < k_1 << 1$ s.t. $|v| < k_1 u$.*

(A3) *The resulting 2DOF maneuvering model can accurately be described by a LPV model.*

As a result, we will in this paper only consider the simplifed 2DOF maneuvering equations given by Davidson and Schiff [2]:

$$M\dot{\nu} + N(u_0)\,\nu = b\delta_R \quad (9)$$

where δ_R is the rudder angle used as control input and $\nu = [v\ r]^\top$ correspond to a body-frame *{B}* located with origin at the center of the ship. Expanded, (9) is written

$$\begin{bmatrix} m - Y_{\dot{v}} & mx_g - Y_{\dot{r}} \\ mx_g - N_{\dot{v}} & I_z - N_{\dot{r}} \end{bmatrix} \begin{bmatrix} \dot{v} \\ \dot{r} \end{bmatrix} + \begin{bmatrix} -Y_v & mu_0 - Y_r \\ -N_v & mx_g u_0 - N_r \end{bmatrix} \begin{bmatrix} v \\ r \end{bmatrix} = \begin{bmatrix} -Y_\delta \\ -N_\delta \end{bmatrix} \delta_R$$

and the entries of the matrices correspond to the (1950) Society of Naval Architects and Marine Engineers (SNAME) notation. This system can, of course, be represented in the traditional linear form $\dot{\nu} = A\nu + B\delta_R$.

We will in the following use nondimensional coefficients which has the advantage of giving an explicit relationship to the

[1] Every point on the curve has an associated tangent circle with radius $\rho = 1/\kappa$. This circle is called the osculating circle.

total speed of the ship $U = \sqrt{u^2+v^2}$ and the ship length L. Nondimensional coefficients are the standard way of expressing the hydrodynamic quantities for ships, since they are independent of ship speed and length, and can therefore be obtained from scaled ship experimental models. In this form, it can be shown that the A-matrix and B-vector can be written

$$\begin{aligned} A &= \begin{bmatrix} a_{11} & a_{12} \\ a_{21} & a_{22} \end{bmatrix} = \frac{U}{L}\begin{bmatrix} a'_{11} & La'_{12} \\ \frac{1}{L}a'_{21} & a'_{22} \end{bmatrix} \\ B &= \begin{bmatrix} b_1 \\ b_2 \end{bmatrix} = \frac{U^2}{L}\begin{bmatrix} b'_1 \\ \frac{1}{L}b'_2 \end{bmatrix} \end{aligned}$$

where the prime $(\cdot)'$ indicates nondimensionality.

A. *Acceleration feedback*

Some recent results [14] show how we can use acceleration feedback to shape the dynamics before we do the control design. In scalar form we can write the dynamical equations as follows

$$\dot{v} = \frac{U}{L}a'_{11}v + Ua'_{12}r + \frac{U^2}{L}b'_1\delta_R + \chi_v \quad (10)$$

$$\dot{r} = \frac{U}{L^2}a'_{21}v + \frac{U}{L}a'_{22}r + \frac{U^2}{L^2}b'_2\delta_R + \chi_r \quad (11)$$

where χ_v and χ_r is our acceleration feedback terms. Define them as follows

$$\chi_v = -a_v\dot{v} \quad (12)$$

$$\chi_r = -a_r\dot{r} \quad (13)$$

which then gives the new LPV system

$$\dot{\nu} = \frac{U}{L}\begin{bmatrix} \frac{a'_{11}}{(1+a_v)} & L\frac{a'_{12}}{(1+a_v)} \\ \frac{1}{L}\frac{a'_{21}}{(1+a_r)} & \frac{a'_{22}}{(1+a_r)} \end{bmatrix}\nu + \frac{U^2}{L}\begin{bmatrix} \frac{b'_1}{(1+a_v)} \\ \frac{1}{L}\frac{b'_2}{(1+a_r)} \end{bmatrix}\delta_R \quad (14)$$

B. *Translating the body-frame*

A useful trick for manipulating a rigid-body dynamics is to translate the body frame within the body-domain. Let the original body-frame be given by $\{B^o\}$ and the new body-frame by $\{B^n\}$. Let the origin of $\{B^n\}$ be located a distance l_x on the x-axis of $\{B^o\}$. If η_3^o, ν_3^o are the original 3DOF position and velocity vectors, and η_3^n, ν_3^n is the new vectors, then they are related by the following equation

$$\eta_3^n = \eta_3^o + l_x R_3(\psi)\varepsilon_1$$

where $\varepsilon_1 = \begin{bmatrix} 1 & 0 & 0 \end{bmatrix}^\top$. This gives

$$\dot{\eta}_3^n = \dot{\eta}_3^o + l_x\dot{R}_3(\psi)\varepsilon_1 = R_3(\psi)\nu_3^o + l_x R_3(\psi)S(r^o)\varepsilon_1$$

where

$$S(x) = \begin{bmatrix} 0 & -x & 0 \\ x & 0 & 0 \\ 0 & 0 & 0 \end{bmatrix}$$

Since $\nu_3^o = R^\top(\psi)\dot{\eta}_3^o$ and $\nu_3^n = R^\top(\psi)\dot{\eta}_3^n$ we get

$$\nu_3^n = \nu_3^o + l_x r^o S(1)\varepsilon_1 = \nu_3^o + l_x r^o \varepsilon_2$$

where $\varepsilon_2 = \begin{bmatrix} 0 & 1 & 0 \end{bmatrix}^\top$. In scalar form this becomes

$$\begin{aligned} u^n &= u^o \\ v^n &= v^o + l_x r^o \\ r^n &= r^o \end{aligned}$$

which give rise to the following linear transformation $\nu_3^n = T\nu_3^o$, where

$$T := \begin{bmatrix} 1 & 0 \\ 0 & T_2 \end{bmatrix}, \text{ and } T_2 := \begin{bmatrix} 1 & l_x \\ 0 & 1 \end{bmatrix}$$

For our 2DOF system, we then get

$$\dot{\nu}^n = T_2\dot{\nu}^o = A_n\nu^n + B_n\delta_R \quad (15)$$

where $A_n = T_2A_oT_2^{-1}$ and $B_n = T_2B_o$. With nondimensional coefficients, we get

$$\begin{aligned} A_n &= T_2AT_2^{-1} \\ &= \frac{U}{L}\begin{bmatrix} a'_{11}+a'_{21}\frac{l_x}{L} & L\left(a'_{12}+(a'_{22}-a'_{11})\frac{l_x}{L}-a'_{21}\frac{l_x^2}{L^2}\right) \\ \frac{1}{L}a'_{21} & a'_{22}-a'_{21}\frac{l_x}{L} \end{bmatrix} \end{aligned}$$

and

$$B_n = T_2B = \frac{U^2}{L}\begin{bmatrix} b'_1 + b'_2\frac{l_x}{L} \\ \frac{1}{L}b'_2 \end{bmatrix}$$

C. *The general dynamical model*

Incorporating both acceleration feedback and translation of the body-frame, we finally obtain the general dynamical LPV model of a ship. Transforming with $\nu = \nu^n = T_2\nu^o$, we get

$$\dot{\nu} = \frac{U}{L}\begin{bmatrix} \bar{a}_{11} & L\bar{a}_{12} \\ \frac{1}{L}\bar{a}_{21} & \bar{a}_{22} \end{bmatrix}\nu + \frac{U^2}{L}\begin{bmatrix} \bar{b}_1 \\ \frac{1}{L}\bar{b}_2 \end{bmatrix}\delta_R \quad (16)$$

where

$$\begin{aligned} \bar{a}_{11} &= \frac{a'_{11}}{1+a_v} + \frac{a'_{21}}{1+a_r}\frac{l_x}{L} \\ \bar{a}_{12} &= \frac{a'_{12}}{1+a_v} + \left(\frac{a'_{22}}{1+a_r} - \frac{a'_{11}}{1+a_v}\right)\frac{l_x}{L} - \frac{a'_{21}}{1+a_r}\frac{l_x^2}{L^2} \\ \bar{a}_{21} &= \frac{a'_{21}}{1+a_r} \\ \bar{a}_{22} &= \frac{a'_{22}}{1+a_r} - \frac{a'_{21}}{1+a_r}\frac{l_x}{L} \\ \bar{b}_1 &= \frac{b'_1}{1+a_v} + \frac{b'_2}{1+a_r}\frac{l_x}{L} \\ \bar{b}_2 &= \frac{b'_2}{1+a_r} \end{aligned}$$

In this resulting model, we can use l_x, a_v and a_r to shape the A-matrix and B-vector to obtain desirable distribution of the elements. We will exploit these extra degrees of freedom in our later design.

Remark 4: The acceleration feedback term χ_v should come from an acceleration measurement (an accelerometer) at the origin of the original body-frame. However, since it is a rigid-body, the location in general makes no difference since measurements from all locations within the ship are related by static maps. Likewise for the χ_r term, but since the yaw rate is the same in both body-frame locations, this makes no difference.

IV. PATH FOLLOWING

Given the kinematic model (6) and the general dynamical model (16) we aim at designing a LAS controller that regulates e_2 and $\bar{\psi}$ to zero, and keeps all other states bounded.

First we need to reduce the kinematics (6) into a suitable 2DOF maneuvering problem. In fact, we wish to only look at the states $X = \begin{bmatrix} e_2 & \bar{\psi} & v & r \end{bmatrix}^\top$. Rewriting (6), we get

$$\dot{\sigma}_0 = F_0^{-1}(e_2, \kappa) R(\bar{\psi}) \nu_3 \tag{17}$$

Let $\xi = \begin{bmatrix} e_2 & \bar{\psi} \end{bmatrix}^\top$ s.t. $\sigma_0 = \begin{bmatrix} s & \xi^\top \end{bmatrix}^\top$ and define $P_2 := \begin{bmatrix} 0 & 1 & 0 \\ 0 & 0 & 1 \end{bmatrix}$ and $P_3 := \begin{bmatrix} 0 \\ P_2 \end{bmatrix}$. Then $P_3^2 = P_3$ and $P_3^\top = P_3$, i.e. P_3 is a valid linear projection. We then have that $\xi = P_2\sigma_0$ and

$$\begin{aligned} \dot{\xi} &= P_2\dot{\sigma}_0 = P_2 F^{-1}(\kappa, \xi) R(\bar{\psi}) \nu_3 \\ &= \begin{bmatrix} \sin(\bar{\psi}) & \cos(\bar{\psi}) & 0 \\ \frac{-\kappa\cos(\bar{\psi})}{1-e_2\kappa} & \frac{\kappa\sin(\bar{\psi})}{1-e_2\kappa} & 1 \end{bmatrix} \begin{bmatrix} u \\ v \\ r \end{bmatrix} \end{aligned} \tag{18}$$

and we want to regulate $\xi \to 0$. In scalar form, the 2 DOF is

$$\dot{e}_2 = u\sin(\bar{\psi}) + v\cos(\bar{\psi}) \tag{19}$$

$$\dot{\bar{\psi}} = \frac{-\kappa}{1-e_2\kappa}\left[u\cos(\bar{\psi}) - v\sin(\bar{\psi})\right] + r \tag{20}$$

$$\dot{v} = \frac{U}{L}\bar{a}_{11}v + U\bar{a}_{12}r + \frac{U^2}{L}\bar{b}_1\delta_R \tag{21}$$

$$\dot{r} = \frac{U}{L^2}\bar{a}_{21}v + \frac{U}{L}\bar{a}_{22}r + \frac{U^2}{L^2}\bar{b}_2\delta_R \tag{22}$$

This model is a generalization of the model used in [6] where the heading and cross-track error is controlled onto a straight-line path. Set $\kappa = 0$, $e_2 = y$, $\bar{\psi} = \psi$ and $\bar{b}_1 = 0$ and then we have recovered the same equations. Elaborating more on that design, Pettersen and Lefeber derive a scalar output map based on the behavior of a helmsman steering a ship onto a straight line path. They claim that

"a good helmsman will use the ship course angle ψ, rather than making the ship glide sideways,..., and the helmsman will choose the magnitude of ψ dependent on the distance from the straight-line, i.e. dependent on y."

Therefore they suggest a desired yaw angle $\psi_d = \rho(y)$ where $\rho : \Re \to \left[-\frac{\pi}{2}, \frac{\pi}{2}\right]$, $\rho(0) = 0$, and $y\rho(y) < 0$. Mapping into $\left[-\frac{\pi}{2}, \frac{\pi}{2}\right]$ ensures that the ship keeps the heading in the direction of the desired motion. One such function ρ is $\rho(y) = -\arctan(y/\varepsilon)$ where ε is a constant used to shape the ship entry onto the straight-line path. From this, they choose the output $z = \psi - \rho(y)$, and obtains the "helmsman" behavior if this output is zero. We will exploit this output redefinition in our design; though, not with output feedback linearization which gives a zero-dynamics of order 2, but rather by using a 3-step backstepping design.

Notice that the system in (19)-(22) is not in strict feedback form, which means that traditional backstepping schemes are not directly applicable. However, we will show a way around this problem, and to do that we will first divide the system into two subsystems, and look at them independently.

A. *Subsystem 1*

For the equation (21) view $\delta_1 = r$ as an input. The next proposition is valid if the following assumption hold

(A4) *The term* $\bar{a}_{11} < 0$ *for* $a_r = 0$ *and* $-1 < a_v < \infty$, *and* $l_x > 0$.

Proposition 1: The system (21) with inputs δ_R and $\delta_1 = r$ and output $y_v = v$ can be made independent of the input δ_R and IOS w.r.t. δ_1 with bound

$$|y_v(t)| \le \beta_1(|v(0)|, t) + \gamma_1(||\delta_1||) \tag{23}$$

where $\beta_1 \in KL$ and linear gain $\gamma_1 < (1-\mu_1)||\delta_1||$, $0 < \mu_1 < 1$.

Proof: Pick the the distance $l_x = -L\frac{(1+a_r)}{(1+a_v)}\frac{b_1'}{b_2'} > 0$. Then $\bar{b}_1 = 0$. Next, with that choice for l_x, pick the acceleration feedback term $a_v = a_v^* = -\dfrac{a_{12}'(b_2')^2 - a_{22}'b_1'b_2' + a_{11}'b_1'b_2' - a_{21}'(b_1')^2}{b_2'(a_{12}'b_2' - a_{22}'b_1')} > -1$ with $a_r = 0$. Then $\bar{a}_{12} = 0$. Since the solution of a_v is continuous in its arguments, there exist a neighborhood around a_v^* s.t. $\bar{a}_{12}$ is small. It can be shown using practical ship model data that *(A4)* holds with these choices of l_x and a_v. The ISS-gain is now bounded by

$$\gamma_1 < L\frac{|\bar{a}_{12}|}{|\bar{a}_{11}|}||\delta_1|| \le (1-\mu_1)||\delta_1||$$

The right-hand inequality allows for small perturbations of $\bar{a}_{12}^*$. ■

Remark 5: Another solution is to pick a_r to cancel $\bar{a}_{12}$ with $a_v = 0$. However, since equipment for measuring angular acceleration is void, we will not use acceleration feedback from $\dot{r}$.

Remark 6: Ideally, we would pick a_v to cancel $\bar{a}_{12}$ exactly, but since the gain is multiplied by $L >> 1$, it is very sensitive to parametric uncertainties. We therefore show that it is sufficient with $\bar{a}_{12} \approx 0$ which gives a small gain γ_1.

B. *Subsystem 2*

For the equations (19), (20) and (22) we will use backstepping to design a suitable control law for δ_R. View $\delta_2 = v$ as a bounded disturbance input satisfying *(A2)*.

B.1 First Step:

Let $z_1 = e_2$ and $z_2 = \bar{\psi} - \alpha_1$. The first recursive step results in the following:

Proposition 2: For the system

$$\dot{z}_1 = u\sin(\alpha_1)\cos(z_2) + u\sin(z_2)\cos(\alpha_1) + \cos(\bar{\psi})\delta_2$$

the virtual control $\alpha_1 = -\arctan\left(\frac{z_1}{\varepsilon}\right)$, $\varepsilon > 0$, with $z_2 = 0$, renders the origin of z_1 L-ISS, and LAS with $\delta_2 = 0$.

Proof: According to *(A2)* define $D_\delta := \{\delta \in \Re \mid |\delta| < k_1 u\}$ s.t. $\delta_2 \in D_\delta$. Let $\Pi_1 = \{z_1 \in \Re \mid |z_1| < z_1^* = (1-\lambda_1)R^*\}$. With the Lyapunov function $V_1 = \frac{1}{2c_1}z_1^2$ we get

$$\dot{V}_1 \le -\frac{1}{c_1}uz_1\sin(\arctan(z_1/\varepsilon)) + \frac{1}{c_1}|z_1||\delta_2(t)|$$

Let $D_1 = \{z_1 \in \Pi_1 |\ z_1 \leq \varepsilon \tan(\arcsin(k_1))\}$ and $B_{1,t} = \left\{z_1 \in \Pi_1 |\ \dot{V}_1(z_1,t) \geq 0\right\} \subset D_1$. Then $V_1 > 0, \forall z_1 \in \Pi_1/\{0\}$, and $\dot{V}_1 < 0,\ \forall |z_1| \in \Pi_1/B_{1,t},\ \delta_2 \in D_\delta$. D_1 is a locally attractive set since $\dot{V}_1 < 0$ on the boundary, and it can be made arbitrarily small by picking ε small enough. ■

Remark 7: As $\varepsilon \to 0$ then $\sin\left(\arctan\left(\frac{z_1}{\varepsilon}\right)\right) \to sgn(z_1)$. In this case we would obtain $\dot{V}_1 \leq -\frac{1}{c_1}(1-k_1)\, u\, |z_1|$ in the proof above.

B.2 **Second Step:**

Let $z_3 = r - \alpha_2$. From the previous step we have, with $z_2 \neq 0$,

$$\begin{aligned} \dot{z}_1 &= -u \sin(\arctan(z_1/\varepsilon)) \cos(z_2) \\ &\quad + u \sin(z_2) \cos(\alpha_1) + \cos(\bar{\psi})\, \delta_2 \qquad (24) \\ \dot{V}_1 &= -\frac{1}{c_1} u z_1 \sin(\arctan(z_1/\varepsilon)) \cos(z_2) \\ &\quad + \frac{1}{c_1} u z_1 \sin(z_2) \cos(\alpha_1) + \frac{1}{c_1} z_1 \cos(\bar{\psi})\, \delta_2 \qquad (25) \end{aligned}$$

Then the next recursive step is given by:

Proposition 3: For the system (24) and

$$\dot{z}_2 = \frac{-\kappa}{1 - z_1 \kappa}\left[u \cos(\bar{\psi}) - v \sin(\bar{\psi})\right] + \alpha_2 + z_3 - \dot{\alpha}_1$$

the virtual control

$$\begin{aligned} \alpha_2 &= -K_p z_2 - \frac{c_2}{c_1} u z_1 \cos(\alpha_1) \\ &\quad + \frac{\kappa}{1 - z_1 \kappa}\left[u \cos(\bar{\psi}) - v \sin(\bar{\psi})\right] + \dot{\alpha}_1 \end{aligned}$$

with $K_p > 0$, and $z_3 = 0$, renders the origin of (z_1, z_2) L-ISpS, and LAS with $\delta_2 = 0$.

Proof: Let $\Pi_2 = \Pi_1 \cup \left\{z_2 \in \Re |\ z_2 < z_2^* = (1-\lambda_2)\frac{\pi}{2}\right\}$. With the Lyapunov function $V_2 = V_1 + \frac{2}{c_2}\sin^2(\frac{z_2}{2})$ we get

$$\begin{aligned} \dot{V}_2 &\leq -\frac{1}{c_1} u z_1 \sin(\arctan(z_1/\varepsilon)) \cos(z_2) \\ &\quad - \frac{1}{c_2} K_p z_2 \sin(z_2) + \frac{1}{c_1} |z_1|\, |\delta_2(t)| \end{aligned}$$

which shows LAS if $\delta_2 = 0$. Define $r_1(x) := 2\varepsilon \tan(\arcsin(\frac{x}{u\cos(z_2^*)}))$ and $r_1^* = r_1(k_1 u)$. Let $d_1 = \frac{u}{c_1}\left[\sin(\arctan(r_1^*/\varepsilon))\cos(z_2^*) - k_1\right]$. For some $d_2 > 0$, small enough, let $r_2 = \arcsin(\frac{c_2 d_2}{K_p})$. Note that we should choose d_2 s.t. $r_2 << z_2^*$. Then $V_2 > 0,\ \forall z_{1,2} \in \Pi_2/\{0\}$, and $\dot{V}_2 < -d_1 |z_1| - d_2 |z_2|,\ \forall |z_{1,2}|_2 > r_1(||\delta_2||) + r_2$. This shows L-ISpS. In fact, let $B_{2,t} = \left\{z_{1,2} \in \Pi_2 |\ \dot{V}_2(z_{1,2}, t) \geq 0\right\}$ and

$$D_2 = \inf_c \left\{ \begin{array}{c} z_{1,2} \in \Pi_2 |\ V_2(z_{1,2}) \leq C \\ \text{s.t. } \forall \bar{z}_{1,2} \in \sup_\tau B_{2,\tau} \Rightarrow V_2(\bar{z}_{1,2}) < C \end{array} \right\}$$

$B_{2,t} \subset D_2$. Then D_2 is a locally attractive set, and its size correspond to the L-ISpS nonlinear gain. ■

Remark 8: Note the restriction $|z_2| < \frac{\pi}{2}$ to avoid that $\cos(z_2) < 0$. Physically, this assumption is interpreted as $\bar{\psi} \in -sgn(e_2) * (0, \pi)$, which means that the ship should be pointing against the path. Close to the path, it can be relaxed since the term $z_2 \sin(z_2)$ would dominate.

B.3 **Last Step:**

Let $z_3 \neq 0$. From the previous step we have (24) and

$$\begin{aligned} \dot{z}_2 &= -\frac{c_2}{c_1} u z_1 \cos(\alpha_1) - K_p z_2 + z_3 \qquad (26) \\ \dot{V}_2 &= -\frac{u}{c_1} z_1 \sin(\arctan(z_1/\varepsilon)) \cos(z_2) - \frac{K_p}{c_2} z_2 \sin(z_2) \\ &\quad + \frac{1}{c_1} z_1 \cos(\bar{\psi}) \delta_2 + \frac{1}{c_2} z_3 \sin(z_2) \qquad (27) \end{aligned}$$

This gives the result of the last step:

Proposition 4: For the system (24), (26) and

$$\dot{z}_3 = \frac{U}{L^2}\bar{a}_{21} v + \frac{U}{L}\bar{a}_{22} r + \frac{U^2}{L^2}\bar{b}_2 \delta_R - \dot{\alpha}_2$$

the control

$$\delta_R = \frac{L^2}{U^2 \bar{b}_2}\left[-K_d z_3 - \frac{c_3}{c_2}\sin(z_2) - \frac{U}{L^2}\bar{a}_{21} v - \frac{U}{L}\bar{a}_{22} r + \dot{\alpha}_2\right]$$

with $K_d > 0$, renders the origin of (z_1, z_2, z_3) LAS with $\delta_2 = 0$. With $\delta_2 \in D_\delta$ it is L-ISpS with bound

$$|z(t)|_2 \leq \beta_2(|z(0)|, t) + \gamma_2(||\delta_2||) + \eta_2 \qquad (28)$$

where $\beta_2 \in KL$, $\gamma_2 \in K$, $\eta_2 \geq 0$. Moreover, the nonlinear gain γ_2 can be made arbitrarily small.

Proof: Let $\Pi_3 = \Pi_2 \cup \{z_3 \in \Re\}$. With the Lyapunov function $V_3 = V_2 + \frac{1}{2c_3} z_3^2$ we get

$$\begin{aligned} \dot{V}_3 &\leq -\frac{u}{c_1} z_1 \sin(\arctan(z_1/\varepsilon)) \cos(z_2) - \frac{K_p}{c_2} z_2 \sin(z_2) \\ &\quad - \frac{K_d}{c_3} z_3^2 + \frac{1}{c_1} |z_1|\, |\delta_2(t)| \end{aligned}$$

which shows LAS if $\delta_2 = 0$. For some $d_3 > 0$, small enough, let $r_3 = \frac{c_3 d_3}{K_d}$. Then $V_3 > 0, \forall z_{1,2,3} \in \Pi_3/\{0\}$, and $\dot{V}_3 < -d_1 |z_1| - d_2 |z_2| - d_3 |z_3|,\ \forall |z_{1,2,3}|_2 > r_1(||\delta_2||) + r_2 + r_3$. This shows L-ISpS. In fact, let $B_{3,t} = \left\{z_{1,2,3} \in \Pi_3 |\ \dot{V}_3(z_{1,2,3}, t) \geq 0\right\}$ and

$$D_3 = \inf_c \left\{ \begin{array}{c} z_{1,2,3} \in \Pi_3 |\ V_3(z_{1,2,3}) \leq C \\ \text{s.t. } \forall \bar{z}_{1,2,3} \in \sup_\tau B_{3,\tau} \Rightarrow V_3(\bar{z}_{1,2,3}) < C \end{array} \right\}$$

$B_{3,t} \subset D_3$. In words, $B_{3,t}$ is the small time-varying blob w.r.t. $\delta_2(t)$ s.t. $\dot{V}_3 \geq 0$ and D_3 is the smallest set with a V_3 levelset as boundary s.t. it contains the worst-case $B_{3,t}$ blob in its interior. Then D_3 is a locally attractive set, and its size correspond to the L-ISpS nonlinear gain.

Let us now look at the region of cenvergence (ROC). We have to look for the largest levelset of V_3 contained in Π_3. Using the coefficients c_1, c_2, c_3 we can form the resulting elipsoids

somewhat arbitrarily in the three directions. The following procedure is suggested: Pick c_2 small. This gives the maximum levelset C^*, by looking at V_3 with $z_1 = z_3 = 0$.

$$C^* = \frac{2}{c_2} \sin^2\left(\frac{z_2^*}{2}\right)$$

where z_2^* was defined in **step 2**. With z_1^* as defined in **step 1** and $z_2 = z_3 = 0$ we get $c_1 = \frac{1}{2C^*} z_1^{*2}$. Finally, we can choose z_3^*. Since $z_3 = r - \alpha_2$ we can e.g. assume that z_3 is bounded by a multiple of u. Then $c_3 = \frac{1}{2C^*} z_3^{*2}$. This ensures a ROC given by

$$D_{z,ROC} = \left\{ z \in \Re^3 | \; V_3(z) \leq C^* \right\}$$

Let $\underline{c} = \frac{1}{4\max(c_1,c_2,c_3)}$ and $\bar{c} = \frac{1}{2\min(c_1,c_2,c_3)}$. Then $\underline{c}|z|_2 \leq V_3(z) \leq \bar{c}|z|_2$. We now get that $\forall\, z(0) \in D_{z,ROC}$ and $\delta_2 \in D_\delta$ then the trajectories will converge to D_3, i.e. $\exists \beta_2 \in KL$, $\gamma_2 \in K$, $\eta_2 \geq 0$, defined on Π_3 s.t. the trajectories are bounded by (28) where $\gamma_2(x) = \sqrt{\bar{c}/\underline{c}}\, r_1(x)$ and $\eta_2 = \sqrt{\bar{c}/\underline{c}}(r_2 + r_3)$. Recall that we can make r_1, r_2 and r_3 arbitrarily small by choosing ε, K_p and K_d appropriately. ■

The resulting closed-loop differential equation for z_3 is given by

$$\dot{z}_3 = -K_d z_3 - \frac{c_3}{c_2} \sin(z_2) \tag{29}$$

Next, we will look at the input/output property of this system.

Corollary 1: The system (24), (26) and (29) with output $y_z = r = z_3 + \alpha_2(z_1, z_2)$ is IOpS with bound

$$|y_z(t)| \leq \bar{\beta}_2(|z(0)|, t) + \bar{\gamma}_2(||\delta_2||) + \bar{\eta}_2 \tag{30}$$

where $\bar{\beta}_2 \in KL$, $\bar{\gamma}_2 \in K$, $\bar{\eta}_2 \geq 0$, defined on Π_3, and $\bar{\gamma}_2$ can be linearly bounded by $\bar{\gamma}_2(x) < (1+\mu_2)||\delta_2||$, $0 < \mu_2 << 1$, $\forall\, \delta_2 \in D_\delta$.

Proof: Doing the algebra, we get to the bound

$$|y_z(t)| \leq \sqrt{1 + K_p^2 + u^2}\, |z|_2 + |\delta_2| + \left[1 + \frac{\kappa^*}{\lambda_1}(1 + k_1)\right] u$$

Then substituting (28) we get

$$\begin{aligned} |y_z(t)| \;\leq\; & \sqrt{1 + K_p^2 + u^2}\, \beta_2(|z(0)|, t) \\ & + \sqrt{1 + K_p^2 + u^2}\, \gamma_2(||\delta_2||) + ||\delta_2|| \\ & + \left[1 + \frac{\kappa^*}{\lambda_1}(1 + k_1)\right] u + \sqrt{1 + K_p^2 + u^2}\, \eta_2 \end{aligned}$$

which gives the bounding functions in (30). Choosing

$$\varepsilon < \frac{\mu_2}{2\sqrt{1 + K_p^2 + u^2}\sqrt{\bar{c}/\underline{c}} \tan\left(\arcsin\left(k_1/\cos(z_2^*)\right)\right)}$$

will ensure the linear bound on $\bar{\gamma}_2$. ■

C. *Interconnecting the subsystems*

Now that we have proven IOpS for both subsystems, we have to see what happens when we interconnect them.

Theorem 1: Let $\delta_1 = y_z = r$ and $\delta_2 = y_v = v$. Then the total system given by (21), (24), (26), and (29) is LAS with total ROC being $D_{vz,ROC} = D_\delta \cup D_{z,ROC}$.

Proof: When $v(0) \in D_\delta$ and $z(0) \in D_{z,ROC}$ then the results in Proposition 1 and Corollary 1 are valid. We look at the bounds (23) and (30) after interconnection, and get

$$\begin{aligned} & ||y_v(t)|| \leq \beta_1(|v(0)|, t) + \gamma_1(||y_z||) \\ & \leq \beta_1(|v(0)|, t) + (1 - \mu_1)\left(\bar{\beta}_2(|z(0)|, t) + \bar{\gamma}_2(||\delta_2||) + \bar{\eta}_2\right) \\ & \leq \beta_1(|v(0)|, t) + (1 - \mu_1)\bar{\beta}_2(|z(0)|, t) \\ & \quad + (1 - \mu_1)(1 + \mu_2)||y_v|| + (1 - \mu_1)\bar{\eta}_2 \end{aligned}$$

and

$$\begin{aligned} & ||y_z(t)|| \leq \bar{\beta}_2(|z(0)|, t) + \bar{\gamma}_2(||\delta_2||) + \bar{\eta}_2 \\ & \leq \bar{\beta}_2(|z(0)|, t) + (1 + \mu_2)\left(\beta_1(|v(0)|, t) + \gamma_1(||y_z||)\right) + \bar{\eta}_2 \\ & \leq \bar{\beta}_2(|z(0)|, t) + (1 + \mu_2)\beta_1(|v(0)|, t) \\ & \quad + (1 + \mu_2)(1 - \mu_1)||y_z|| + \bar{\eta}_2 \end{aligned}$$

Finally, design μ_1 and μ_2 s.t. $(1 + \mu_2)(1 - \mu_1) < \mu < 1$. ■

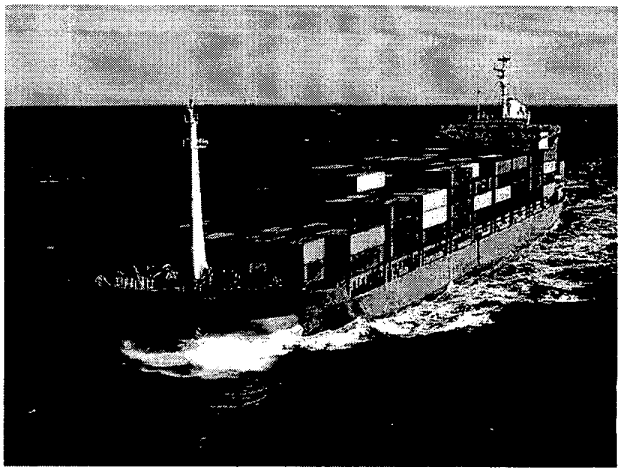

Fig. 3. Container ship. Courtesy: http://www.bremen-ports.de/gallery/pics

V. CASE STUDY

We will consider a container ship with data given in the new *Matlab® GNC toolbox* [15]. The ship length is $L = 175\,\mathrm{m}$, and service speed is $u_0 = 10\,\mathrm{m/s}$. The nondimensional coefficients are $a'_{11} = -0.7072$, $a'_{12} = -0.2860$, $a'_{21} = -4.1078$, $a'_{22} = -2.6619$, $b'_1 = -0.2081$ and $b'_2 = 1.5238$. These data are taken from a well documented containership and is found in the command *Lcontainer.m* in the *GNC* toolbox. Let $a_r = 0$. This gives $a_v = -0.7334$ and $l_x = 89.63\,\mathrm{m}$. Notice that the body-frame with this l_x is moved just ahead of the ship bow. This is not a problem since this can be taken into account by the guidance system.

A turning circle trial for this ship can be run using the *Matlab®* script *ExTurnCircle.m*, see figure (4), and this gives the design parameter: *Steady turning radius :* $695\,\mathrm{m}$ .Therefore, we set the minimum radius $R^* = 700\,\mathrm{m}$ and $\kappa^* = 0.0014$. The

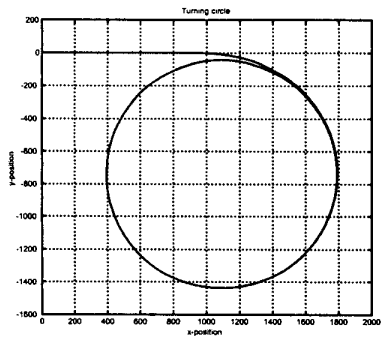

Fig. 4. The *Matlab*® *GNC* command ExTurnCircle.m executes a turncircle trial on the containership to obtain important design parameters.

following simulation has been done with the initial condition $\left[e_2(0)\ \bar{\psi}(0)\ v(0)\ r(0)\right]^\top = [1\,\mathrm{m}, -5\,^\circ, 0.2\,\mathrm{m/s}, 0.5\,^\circ/\mathrm{s}]$, $K_p = 0.1$, $K_d = \frac{u^2}{(10L)^2}$ and $\varepsilon = 0.8$. With the choices $z_1^* = 642.9\,\mathrm{m}$, $z_2^* = 0.45\pi$ and $z_3^* = 0.5$ we got the value for the largest levelset $C^* = 2.812$ and $c_1 = 7.349 \cdot 10^{-4}$, $c_2 = 0.300$ and $c_3 = 0.0445$. Then $V_3(z(0)) = 1.4076 < C^*$. Moreover, $k_1 = 0.1$ and $v(0) = 0.2 < k_1 u_0$.

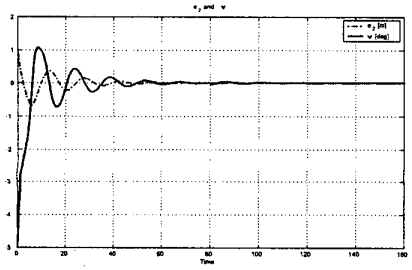

Fig. 5. Plot of the states e_2 and $\bar{\psi}$ which are seen to converge close to zero.

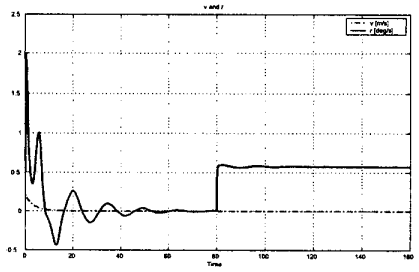

Fig. 6. Simulation plot of the states v and r. In simulation, v was decoupled from the rest of the system and is seen to exponentially converge to zero.

The simulation was done using *Matlab*® and *Simulink*®. Initially, the ship was controlled to follow a straight line with $\kappa = 0$. At $t = 80\,\mathrm{s}$ the curvature was switched to $\kappa = 0.001$ which explains the jump in r. A caveat in this simulation was that the rudder was assumed unrestricted. In real life it would therefore be heavily saturated. However, if we redesign the controller by adding some extra variables to play with, or more exact, let $\alpha_1 = -\Delta \arctan(z_1/\varepsilon)$ and $K_z z_3 = r - \alpha_2$, then simulation has shown that by playing with Δ and K_z we can avoid saturation. This is the scope of future research.

VI. Conclusion

We have in this paper addressed control design for maneuvering ships onto curves in the plane. In that context, we have used the Serret-Frenet frame to identify the error signals, i.e. the cross-track error e_2 and the yaw error $\bar{\psi}$, corresponding to the curve. We have briefly introduced some notions of curve theory to illustrate how the equations appear. A good contribution is given in the manipulation of the dynamical equations by introducing acceleration feedback and by moving the body-frame. Finally we have developed a controller for the path-following problem based on three steps of backstepping and interconnection of subsystems. Simulations show that the controller works well; however, a caveat is at this point heavy saturation of the rudder.

Future work will be to look into other design strategies, to remove saturation, to introduce environmental disturbances and robustify the design, and to include observers to estimate unmeasured states. Moreover, a large amount of work lies in designing a well-working guidance system.

References

[1] Thor I. Fossen, "A Survey on Nonlinear Ship Control: From theory to practice.," in *Proc. 5th IFAC Conf. Manoeuvering Control Marine Crafts*, Aalborg, Denmark, Aug. 2000, International Federation of Automatic Control, pp. 1–16.

[2] K. S. M. Davidson and L. I. Schiff, "Turning and Course Keeping Qualities," *Trans. Soc. of Nav. Architects Marine Eng.*, vol. 54, 1946.

[3] K. Nomoto, T. Taguchi, K. Honda, and S. Hirano, "On the Steering Qualities of Ships," Technical report 4, Int. Shipbuilding Progress, 1957.

[4] T. Holzhüter, "LQG approach for the high-precision track control of ships," *IEE Proc.Control Theory Appl.*

[5] Thor I. Fossen, *Guidance and Control of Ocean Vehicles*, John Wiley & Sons Ltd., England, 1994.

[6] K.Y. Pettersen and E. Lefeber, "Way-point tracking control of ships.," To appearn in Proc. 40th IEEE Conf. Decision & Control, Dec 2001.

[7] R. Zhang, Y. Chen, Z. Sun, F. Sun, and H. Xu, "Path Control of a Surface Ship in Restricted Waters Using Sliding Mode," in *Proc. 37th IEEE Conf. Decision & Control*, Tampa, Florida, USA, Dec 1998, pp. 3195–3200.

[8] P. Encarnação, A. Pascoal, and M. Arcak, "Path Following for Autonomous Marine Craft.," in *Proc. 5th IFAC Conf. Manoeuvering Control Marine Crafts*, Aalborg, Denmark, Aug. 2000, International Federation of Automatic Control, pp. 117–122.

[9] P. Encarnação and A. Pascoal, "3D Path Following for Autonomous Underwater Vehicle.," in *Proc. 39th IEEE Conf. Decision & Control*, Sidney, Australia, Dec. 2000, Institute of Electrical and Electronics Engineers, pp. 2977–2982.

[10] Hassan K. Khalil, *Nonlinear Systems*, Prentice-Hall, Inc., New Jersey, 2 edition, 1996.

[11] Z.-P. Jiang, A. R. Teel, and L. Praly, "Small-gain theorem for ISS systems and applications," *Math. Control Signals Systems*, vol. 7, no. 2, pp. 95–120, 1994.

[12] Olav Egeland and Jan Tommy Gravdahl, "Modeling and Simulation for Control.," Lecture Notes 2001-1-X, Norw. Univ. Sci. & Tech., Trondheim, Norway, Jan 2001.

[13] M. M. Lipschutz, *Schaum's outline of Theory and Problems of DIFFERENTIAL GEOMETRY*, McGraw-Hill Book Company., New York, 1969.

[14] Thor I. Fossen, Karl-Petter Lindegaard, and Roger Skjetne, "Inertia shaping techniques for marine vessels using acceleration feedback," Submitted to Proc. 15th IFAC World Congress Automatic Control, July 2002.

[15] Thor I. Fossen, "Matlab GNC Toolbox, Marine Cybernetics.," Internet, August 1, 2001, <http://www.marinecybernetics.com>.